8-1-2014

A Probabilistic Tsunami Model For Chile

Vaclav Rara

Cristina Arango

Petr Puncochar

Goran Trendafiloski

Chris Ewing

See next page for additional authors

Authors
Vaclav Rara, Cristina Arango, Petr Puncochar, Goran Trendafiloski, Chris Ewing, Adam Podlaha, Deepak Vatvani, and Maarten Van Ormondt

11th International Conference on Hydroinformatics
HIC 2014, New York City, USA

A PROBABILISTIC TSUNAMI MODEL FOR CHILE

VACLAV RARA (1), CRISTINA ARANGO (2), PETR PUNCOCHAR (1), GORAN TRENDAFILOSKI (2), CHRIS EWING (2), ADAM PODLAHA (2), DEEPAK VATVANI (3), MAARTEN VAN ORMONDT (3), AND ADRIAN CHANDLER (4)
(1): Impact Forecasting, Aon Benfield, Vaclavske namesti 19, Prague, 110 00, Czech Republic
(2): Impact Forecasting, Aon Benfield, 55 Bishopsgate, London, EC2N 3BD, England (UK)
(3): Deltares, Rotterdamseweg 185, Delft, 2600, Netherlands
(4): Aon Benfield UCL Hazard Centre, Gower Street, London, WC1E 6BT, England (UK)
Email contact: vaclav.rara@aonbenfield.com

KEY WORDS: Chile, probabilistic model, earthquake, tsunami, insurance, NAT-CAT model

ABSTRACT: In earthquake and tsunami risk-prone regions such as Chile, catastrophe models help insurers and reinsurers understand and quantify the potential financial losses caused by these perils. The 2010 Maule earthquake highlighted the need for quantifying losses not only from primary perils (earthquake) but also from secondary perils such as tsunamis, which contribute to the overall event losses but are not often modelled.
This paper describes the methodology and application behind a new earthquake and tsunami catastrophe model for Chile developed by Impact Forecasting in collaboration with its Aon Benfield Research partners. The Chile earthquake and tsunami model is validated through comparison of the modelled and observed losses for client portfolios from the 2010 event.

1. INTRODUCTION

A tsunami is a natural phenomenon consisting of a series of waves that are generated by a rapid displacement of a large volume of water in the sea or in the lake [16, 20]. Displacements of large volumes of water can be generated by earthquake rupture which can induce vertical uplift (displacement) of seabed, submarine landslides or volcanic eruptions. This paper focuses on the tsunamis induced by earthquakes and the modeling of their potential financial impacts. Disastrous tsunamis are relatively rare events and are known for their devastating impact on the coast, capacity to inundate large territories, and for causing high property damage, physical injuries and fatalities.

In order to quantify the potential loss of property and life arising from major catastrophic events, such as earthquakes and induced tsunamis, the (re) insurance industry uses tool/techniques referred to as catastrophe models. The output from a catastrophe model is a curve indicating the probabilities of exceeding different levels of loss, also called an Exceedance Probability Curve (EP curve). The calculation of an EP curve involves a probabilistic approach in which thousands of events are simulated and the damage and related loss stemming from each of these events is calculated.

This paper presents some key modelling aspects of a new catastrophe model for Chile developed by Impact Forecasting in collaboration with Aon Benfield Research partners, focusing on the tsunami component. The model has the capability to model tsunami as a secondary peril – losses due to earthquake (ground-shaking) and induced tsunamis along the Chilean coast are quantified in a probabilistic manner, and also for historical scenarios. The model is implemented in the IF catastrophe-modelling platform, ELEMENTS.

The process of tsunami modelling consists of the simulation of three main phases: wave generation, wave propagation and inundation. Out of these three phases, only the propagation phase can be accurately modelled and considered to be properly understood [16, 20].

TSUNAMI GENERATION

The two most common forms of tsunami generation [16, 20] are coseismic displacement associated with earthquake rupture and mass failures (such as submarine landslides). Coseismic displacement tends to generate tsunamis with longer wave lengths above larger source areas than those generated by mass failures, which generally produce tsunamis that attenuate more rapidly.

WAVE PROPAGATION

The second phase involves the propagation of the tsunami through the open and deep ocean (not being affected by the sea bed) and can be modelled by several approaches. One of the methods for open and deep sea propagation is performed using linear long-wave equations. This method is implemented into modelling suite Delft3D (Deltares) [5] to achieve a high level of simulation accuracy and effectiveness.

INUNDATION

Inundation, as the last phase, is the most complex and difficult phenomenon to understand and to model [4]. Shallow water equations [3] (also known as Saint Venant equations) derived from the depth-integrating Navier-Stokes equations, are used to simulate tsunami wave propagation through areas of shallow sea and through inland inundation. Delft3D-FLOW, which solves these equations for an incompressible fluid, under the Boussinesq assumptions is used in a 2-dimensional setting considering a non-steady flow regime. A numerical solver applies a flooding scheme based on the work of Stelling and Duinmeijer, (2003). The scheme is designed for rapidly varying depth-averaged flow as occurs, for instance, during dry land inundation or flow transitions due to large gradients of the bathymetry [6].

2. INPUT DATA

Perils such as fluvial or pluvial flooding, tsunamis or dam-break, require detailed and accurate topographical data to capture the natural variation and diversification of such perils across a fine spatial resolution.

Global datasets commonly used for earthquake catastrophe models do not provide sufficient levels of detail, while details gained from LiDAR-based digital terrain models would require non-realistic computing requirements, which in the case of probabilistic modelling play an important role. Last but not least, LiDAR or similarly detailed data, offer, an often incomplete coverage particularly outside of urban areas. The Shuttle Radar Topography Mission (SRTM) dataset [7] with its native resolution of ~90m (around equator) is a reasonable compromise between preserved accuracy and the run time factor. This dataset incurred during the NASA Endeavour mission in 2000, is suitable for the country-wide natural-catastrophe modelling for (re)insurance purposes.

The availability of datasets describing the ocean floor is more complicated. The range of bathymetry datasets is significantly smaller than datasets for land surface. General Bathymetric Chart of the Oceans (GEBCO) [10] represents one of the few suitable options. The bathymetry data were produced by combining the published Smith and Sandwell global topographic grid between latitudes 80°N and 81°S (version 11.1, September, 2008) with a database of over 290 million bathymetric soundings. The resolution of 30 arc-second (approximately 1km) is considerably coarser but is the only option for a global dataset with coverage across the entire area of interest.

Connecting the two datasets could cause significant disturbance and can ultimately lead to instabilities during the numerical simulation. Manual correction was required to connect these two datasets, and the final digital model consisting of SRTM and GEBCO was used for the model set-up and hydrodynamic simulation.

To minimize computational requirements, some areas with no financial exposure were excluded from the overall simulation as the final effect on loss estimates remains unchanged. A classification of urban zones was carried out combining the global land-cover dataset, manual classification of satellite imaginary and geo-coded, market-wide, insurance exposure.

3. MODEL DEVELOPMENT

Catastrophe models generally contain the following components: (1) Hazard, (2) Vulnerability (3) Exposure, and (4) loss. The hazard component represents the frequency and severity of the peril with regards to spatial and temporal data. In the case of earthquakes-induced tsunamis, this refers to the frequency of tsunamigenic events and their severity. The vulnerability component classifies the susceptibility of the portfolio to the hazard. For property (re) insurance the building type, main use, construction material, age, etc., may all be modelled to try to give an accurate description of the building. The exposure data represents the information within the risk portfolio, such as total insured values (TIVs), deductible and limit information and reinsurance application. The loss component calculates financial losses based on information supplied in the exposure data.

3.1. HAZARD COMPONENT: TSUNAMIGENIC EVENTS

Along the Chilean coast, great (M > 8.0) earthquakes are generated when large areas of the subduction rupture. This process can give rise to large tsunamis such as those produced by the 1960 Valdivia (M=9.5) and 2010 Maule (M=8.8) earthquakes. The size and destructive potential of tsunamis that often follow large offshore earthquakes is determined by the amount and area of vertical uplift of the seabed and these two factors are sensitive to the geometry of the slipping fault (i.e., orientation, dip, and depth).

The probabilistic modelling of earthquake-induced tsunamis for Chile is based on simulated earthquakes (stochastic event set) that are consistent with the seismic (ground-shaking) hazard developed for the region (Figure 3.1a). This stochastic tsunami event set represents thousands of simulations of earthquake occurrence patterns in the region. In this study, the seabed vertical displacement resulting from each of the stochastic events has been calculated in order to define the tsunami generation phase. The orientation, dip, and depth of these stochastic earthquake ruptures have been randomised, producing a range of vertical seabed uplifts for a given earthquake magnitude, as shown in Figure 3.1b. This was done in order to capture variation in earthquake characteristics and the resulting slip.

The RuptGen software by Babeyko (2007) was used to calculate the seabed vertical displacement resulting from earthquake slip at depth. The co-seismic displacement is modelled according to the classical Okada (1985) model assuming an uniform-slip rectangular rupture in a homogeneous half-space (Figure 3.1d).

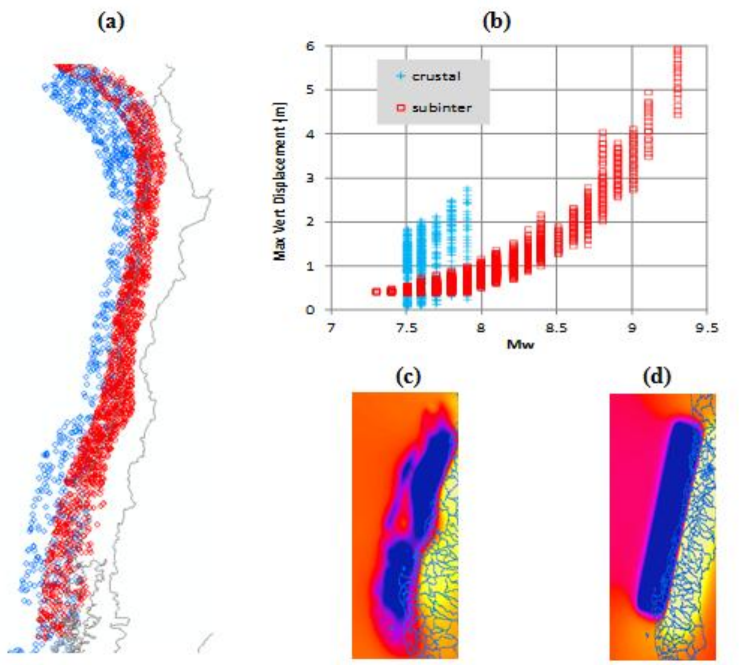

Figure 3.1 (a) Stochastic events modeled along the Chilean coast showing oceanic crust (blue points) and subduction events (red points) generated. (b) maximum seabed vertical displacement generated by events of different magnitudes. (c) distribution of vertical uplift for a non-uniform distribution - 2010 Maule Chilean earthquake and (d) assuming a uniform slip. (source: Aon Benfield)

More than 3,600 events were selected for tsunami simulations, which include both subduction events as well as moderate-size earthquakes occurring in the oceanic crust (Figure 3.1a). Criteria for selecting tsunamigenic events were developed based on the amount and area of vertical displacement generated by each event and considering different locations along the Chilean coast. Thus test runs involving wave propagation and inundation analyses for different events giving rise to different vertical uplifts, were undertaken in order to define a threshold of displacement below which inundation depths at the coast were negligible. Stochastic events below these thresholds were regarded as not having a tsunami generation potential.

3.2. DELFT3D SET UP

Because of its length, modeling tsunamis along the Chilean coast can be a complex and time-consuming procedure. To process the hydrodynamic simulation, a three-level domain hierarchy with different resolutions was chosen. The smaller domains are more computationally efficient than large domains, with much more effective work with CPU memory particularly in 32bit software.

More than 4,000 km of the Chilean coastline is covered as follows:
(i) By 1 first-level domain with a grid resolution of 2000 by 2000 meters
(ii) By 20 second-level domains with a grid resolution of 450 by 450 meters
(iii) By 217 third-level domains with a grid resolution of 90 by 90 meters

The entire hierarchical domain set-up uses a nesting procedure (Figure 3.2.1). First, the 1st level domains with the coarsest resolution are processed, with the static vertical displacement of the tsunamigenic event taken as the initial conditions. Then, the 2nd level domains are simulated while taking the 1st level domain model simulation results as the time-dependent boundary conditions. In the last step, the 3rd level domains with the finest resolution are set up using results from the 2nd order, model simulations in exactly the same way as in the second step.

Generally, there are two approaches on how to apply roughness in inundation modeling. The first is a model that uses a uniform roughness coefficient for the whole computational domain and second which uses a very detailed roughness and land cover datasets. A detailed roughness approach is usually used when the obstacle or urban use (e.g., buildings, sea-walls, roads) is represented adequately within grid cells in the inundation model.
Due to uncertainties in the process of the tsunami roughness assessments, and considering roughness is changing in time as the tsunami wave fluctuates and approaches inland with various changes in landscape affecting the hydraulic roughness, detailed literature review [1,4,9,14] and expert consultancy preceded the final roughness setting. Finally, it was concluded, due to the spatial resolution of the DEM and the global land cover datasets, to use constant Manning's roughness coefficient 0.02 for the sea bed and 0.035 for land.
Validation of the model set-up, and the resulting tsunami flood extent against 2010 event's surveyed extent (section 4) confirmed that the roughness setting is within acceptable limits.

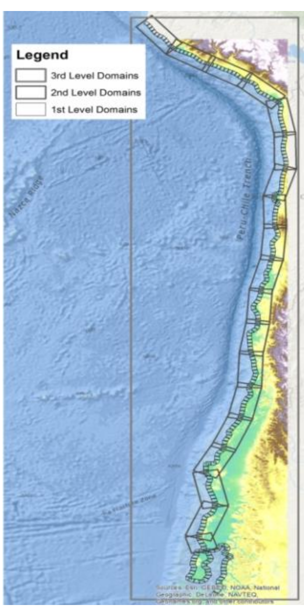

Figure 3.2.1 Nesting of the domains (source: GEBCO, Aon Benfield)

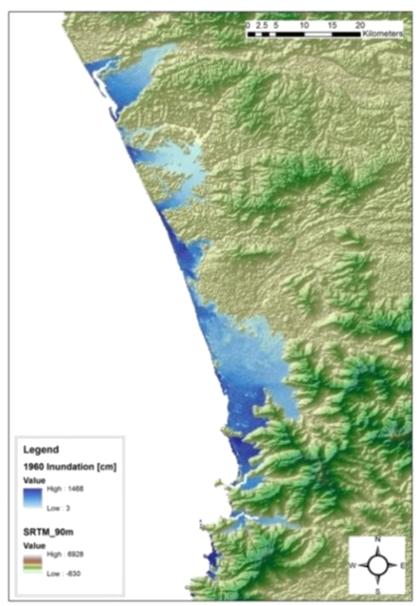

Figure 3.2.2 Tsunami extent for 1960 event (source: SRTM, Aon Benfield)

3.3. VULNERABILITY

The main purpose of the vulnerability component is to calculate the potential damage to affected exposures. The main part of the component is the database of damage curves in which the damage expressed as mean damage ratio is correlated to inundation depth. The mean damage ratio represents the property cost-replacement factor experiencing a certain damage level.

The database contains: (1) damage curves for 24 structural types and 21 general and detailed occupancies; (2) damage curves for buildings, contents and business interruption. Building damage curves (Figure 3.3) are developed by correlating building resistance calculated from the Chilean seismic design code to tsunami horizontal quasi-static water pressure. Contents damage and business interruption curves are based on the corresponding HAZUS damage and business restoration time curves for detailed occupancies [11].

The damage uncertainty is introduced by standard deviation of the beta distributed mean damage ratio.

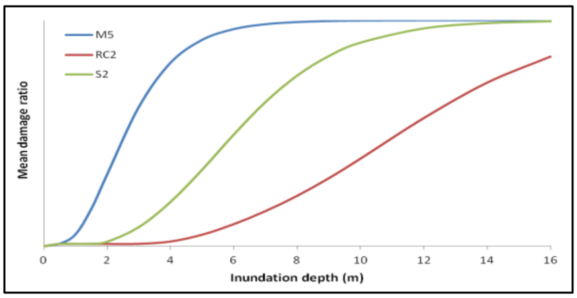

Figure 3.3 Examples of building damage curves for Chile for different construction types: M5 – Overall strengthened masonry; RC2 – RC shear walls; S2 – Steel braced frame (source: Aon Benfield)

4. VALIDATION

On Saturday, 27 February 2010, at 03:34 local time, an earthquake of 8.8 magnitude struck the offshore of the Maule in central Chile. Occurring along the interface between the Nazca and South American plates, this subduction zone event caused severe ground shaking across a 660 km (400 miles) area and generated a tsunami that ravaged the coastline. 521 people were killed and the economic loss stood at US$ 30 billion [13].

Hazard

Validation of the tsunami hazard (e.g., tsunami extent) is, in principle, very complicated because of the lack of observed data. Mankind has a relatively rich history of tsunami records going back more than 1000 years [12,18]. However, a spatially continuous description of the inundation (tsunami extent, recorded maximum depths or even peak velocity) is usually missing. Although, in the past 60 years, survey methods has improved significantly and several tsunamigenic earthquakes happened, only three serious tsunami events were mapped in more detail: 2004 Sumatra, 2010 Chile and 2011 Japan [2,8,15,17,19].

Tsunami hazard for the Chilean model was validated against real, surveyed extent from the 2010 event [2,8]. However, even such a recent and destructive event is surveyed discretely, basically only a few locations along the coast are documented, thereby allowing practical validation. This makes the conclusions of a global validation limited. Figure 4.1 shows a comparison of the simulated extent (shaded blue area) with real observed extent (red line) for 2010 event.

Vulnerability and losses

The 2010 tsunami was triggered by a near-source earthquake and the observations contained aggregate earthquake + tsunami loss. This implies that in many locations it was impossible to identify the loss amount caused by the tsunami only, thus making the validation of the tsunami vulnerability component very hard. However, the aggregated loss was validated by running jointly the earthquake and tsunami components of the model, as Figure 4.2 demonstrates.

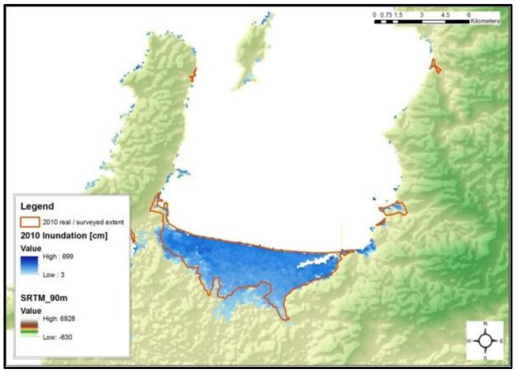

Figure 4.1 Validation of the tsunami hazard component – Talcahuano area, 2010 event (source: GEER team report; Aon Benfield)

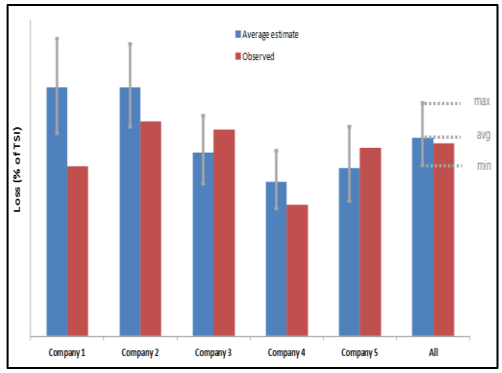

Figure 4.2 Validation of the model - losses (source: Aon Benfield)

5. DISCUSSION

Every catastrophe model, as with any other model, represents a certain simplification of natural behavior. In this case a very complex and inter-disciplinary phenomenon is being described and modelled and therefore a deep understanding of the entire approach is essential, including its strongest features, as well as its limitations.

More than 3,600 events were selected for tsunami simulations, which include both subduction events as well as moderate-size earthquakes occurring in the oceanic zone. Criteria for selecting tsunamigenic events were developed based on the amount and area of vertical displacement generated by each event, and considering different locations along the Chilean coast.

As the 90m resolution for the probabilistic tsunami modelling of this scale is rather detailed, some small natural and (especially) man-made structures can be missed. In extreme situations, this can cause differences from reality, which can affect the resulting extents and related losses.

Methods applied to describe the on-shore tsunami flood extents follow the latest development in scientific approaches but still they can’t capture all aspect of tsunamis, such as time-depended changes in hydraulic roughness, effect of the momentum of transported debris, or (looking on a smaller scale) the use of tsunami predictions and warning systems (e.g. evacuation plans).

6. CONCLUSIONS

Potential losses for the insurance industry will rise as the insurance penetration in the Chilean market increases, as well as the wealth accumulation in vulnerable areas. Probabilistic earthquake and tsunami models can significantly help insurance and risk sectors to better understand the risks that they face. This can lead to a better understanding of catastrophe risk insurance pricing.

Extensive validation of each individual model component and the successful comparison of modelled and observed historical losses from event 2010, show a good description of the real behavior of the tsunami phenomenon.

REFERENCES

[1] Aburaya T., Imamura F. "The proposal of a tsunami runup simulation using combined equivalent roughness," *Annual Journal of Coastal Engineering, Japan Society of Civil Engineers, Vol.49, pp. 276-280,* (2002)

[2] Bray J., Frost D., et al, "Geo-engineering Reconnaissance of the 2010 Maule, Chile Earthquake", *Report of the NSF Sponsored GEER Association Team, version 2,* (2010)

[3] Chow Ven Te, "Open-Channel Hydraulics", (1959)

[4] Dalrymple, R. A., Grilli, S. T., and Kirby, J. T., "Tsunamis and challenges for accurate modeling, Advances in Computational Oceanography", (2006)

[5] Deltares, http://www.deltaressystems.com/hydro/product/621497/delft3d-suite

[6] Deltares: Delft3D-Flow user manual, (2011)

[7] Farr, T. G., et al., "The Shuttle Radar Topography Mission", *Rev. Geophys., 45, RG2004, doi:10.1029/2005RG000183*, (2007)

[8] Fritz H.M., et al, "Field Survey of the 27 February 2010 Chile Tsunami", *Pure and Applied Geophysics*, (2011)

[9] Gayer G., Leschka S., Nöhren I., Larsen O. and Günther H., "Tsunami inundation modelling based on detailed roughness maps of densely populated areas", *Natural Hazards and Earth System Sciences*, (2010)

[10] GEBCO, *http://www.gebco.net*

[11] HAZUS-MH, Multi-hazard Loss Estimation Methodology, Flood model, Federal Emergency Management Agency (2010)

[12] Historical Tsunami Databases for the World Ocean, Institute of Computational Mathematics and Mathematical Geophysics. Novosibirsk, Russia

[13] Impact Forecasting, "Annual Global Climate and Catastrophe Report 2010", (2011)

[14] Kaiser G., Scheele L., Kortenhaus A., Løvholt F., Römer H. and Leschka S., "The influence of land cover roughness on the results of high resolution tsunami inundation modeling", *Natural Hazards and Earth System Sciences*, (2011)

[15] Kawata Y., Tsuji Y. et al, "Comprehensive analysis of the damage and its impact on coastal zones by the 2004 Indian Ocean tsunami disaster", *Research supported by Grant-in-Aid for Special Purposes Research Report , Ministry of Education, Culture, Sports, Science and Technology of Japan*, (2005)

[16] Levin B., Nosov M. "Physics of Tsunamis", (2009)

[17] Mori, N. et al., 2011. "Survey of 2011 Tohoku earthquake tsunami inundation and run-up," *Geophysical Research Letters, Vol. 38,* (2011)

[18] National Geophysical Data Center / World Data Service (NGDC/WDS): Global Historical Tsunami Database. National Geophysical Data Center, NOAA. doi:10.7289/V5PN93H7

[19] Sugawara D., et al., "Initial field survey report of the 2011 East Japan Tsunami in Sendai, Natori and Iwanuma Cities" (2011)

[20] Tiampo, Kristy F., Weatherley, Dion K., Weinstein, Stuart A., "Earthquakes: Simulations, Sources and Tsunamis", (2008)